Atmos. Meas. Tech. Discuss., https://doi.org/10.5194/amt-2019-119
Manuscript under review for journal Atmos. Meas. Tech.
Discussion started: 12 April 2019

Atmospheric Measurement Techniques Discussions

A comparison of lognormal and gamma size distributions for characterizing the stratospheric aerosol phase function from OPC measurements

Ernest Nyaku[1], Robert Loughman[1], Pawan K. Bhartia[2], Terry Deshler[3], Zhong Chen[4], and Peter R. Colarco[2]

[1]Center of Atmospheric Science, Hampton University, Hampton
[2]NASA Goddard Space Flight Center, Greenbelt, Maryland, 20771, USA
[3]Department of Atmospheric Science, University of Wyoming, Laramie, Wyoming
[4]Science Systems and Applications, Inc. (SSAI), 10210 Greenbelt Road, Suite 600, Lanham, Maryland 20706, USA

Correspondence: Ernest Nyaku (ernest.nyaku@hamptonu.edu)

Abstract.

A series of in situ measurements made by optical particle counters (OPC) at Laramie, Wyoming provides size-resolved stratospheric aerosol concentration data for the period of 2008-2017. These data are analyzed in this study for the purpose of assessing the sensitivity of the stratospheric aerosol phase function to the aerosol size distribution (ASD) model used to fit the measurements. The two unimodal ASD models investigated are the uni-modal lognormal (UMLN) and gamma distribution models, with the minimum χ^2 method employed to assess how well each ASD fits the measurements. The aerosol phase function (APF) for each ASD is calculated using Mie theory, and is compared to the APF derived from the Community Aerosol and Radiation Model for Atmospheres (CARMA) sectional aerosol microphysics module. Comparing the χ^2 values for the fits at altitudes 20 km and 25 km shows that the UMLN distribution better represents the OPC measurements. The importance of data at aerosol radius below 0.1 $\mu\mathrm{m}$ is also demonstrated: When these data are not available from OPC measurements, the gamma distribution provides a more stable derived APF. The gamma distribution also fits the CARMA model results better than the UMLN model, when the CARMA model results are binned to mimic the OPC measurement bins (and therefore measurements between 0.05 and 0.1 $\mu\mathrm{m}$ are excluded).

1 Introduction

The presence of aerosol particles in the stratosphere has significant impact on atmospheric dynamics, atmospheric chemistry, and climate by altering the amount of radiation that reaches the Earth's surface, as research over the past few decades has shown (Kremser et al., 2016). These aerosols form a layer of liquid droplets that are a mixture of sulfuric acid (H_2SO_4) and water (H_2O), discovered by Junge in 1960 (Junge et al., 1961). They can cool the Earth's surface and troposphere by scattering incoming short-wave radiation and warm the lower stratosphere by absorbing outgoing long-wave radiation (Robock, 2000; Kravitz et al., 2011; Ridley et al., 2014). These aerosols found in the stratosphere act as condensation nuclei for polar stratospheric clouds (PSCs), which provide a surface for heterogeneous chlorine activation and denitrification processes leading to

Atmos. Meas. Tech. Discuss., https://doi.org/10.5194/amt-2019-119
Manuscript under review for journal Atmos. Meas. Tech.
Discussion started: 12 April 2019

Atmospheric Measurement Techniques Discussions

ozone depletion (McCormick et al., 1995; Andreae and Crutzen, 1997; Solomon, 1999). The main sources of the stratospheric aerosols as summarized by Kremser et al. (2016) are from sulfur dioxide (SO_2) and carbonyl sulfide (OCS), which are both oxidized to sulfuric acid. OCS originates from marine sources and is transported by convection into the tropical stratosphere from the troposphere. Through large volcanic eruptions, SO_2 is also injected directly into the stratosphere leading to an increased aerosol concentration that lasts for several years as was observed after the eruptions of El Chichón (Mexico, 1982) and Pinatubo (Philippines,1991).

The stratospheric aerosol phase function $P_a(\Theta)$ describes the angular distribution of the scattered solar radiation and it depends on the size, shape, and refractive index of the aerosol. The value of the phase function for a given scattering angle is proportional to the probability that an incident photon will be scattered in a particular direction. The $P_a(\Theta)$ is calculated from the aerosol size distribution (ASD) using Mie theory (Deirmendjian, 1969). Here we make the assumption that the aerosol particles in the stratosphere are spherical and homogeneous and apply a refractive index which is appropriate for sulfuric acid. The aerosol phase function (APF) is needed to accurately interpret limb scatter (LS) measurements (von Savigny et al., 2015; Rault and Loughman, 2007), or LIDAR measurements, to yield extinction estimates, but not for satellite measurements which use occultation. The actual ASD varies in space (latitude,longitude, and altitude) and time, but scattering based retrievals rarely include this variation.

The Ozone Mapping and Profiler Suite, Limb Profiler (OMPS/LP) (Jaross et al., 2014; Rault and Loughman, 2013; Flynn et al., 2006), the Optical Spectrograph and InfraRed Imaging System (OSIRIS) (Llewellyn et al., 2004) and Scanning Imaging Absorption spectroMeter for Atmospheric CartograpHY (SCIAMACHY) (Bovensmann et al., 1999) are three limb scattering instruments that have been mounted on satellite platforms to measure limb scattered sunlight. These satellite instruments have measured the limb radiance profiles from wavelengths ranging from the UV to the near infrared from which stratospheric aerosol extinction profiles, the standard operational product (for OMPS/LP and OSIRIS) are retrieved. The retrieval of stratospheric aerosol extinction profiles from limb radiance measurements (Rault and Loughman, 2007; Bourassa et al., 2007, 2008; Taha et al., 2011; Ovigneur et al., 2011; Bourassa et al., 2012; Ernst, 2013; von Savigny et al., 2015; Rieger et al., 2015, 2018; Loughman et al., 2018), involves the comparison of measured limb radiance data with simulated radiances that are generated by radiative transfer (RT) models. This approach has also been used to obtain the ASD information of stratospheric aerosol from limb scatter measurements (Malinina et al., 2018).

Several ASDs that are used in the aerosol extinction retrieval algorithms by the various LS instruments are presented in Table 2 of Loughman et al. (2018). In many cases, the assumed size distributions used for the derivation of the phase functions are based on lognormal distribution fits made to the University of Wyoming OPC measurements at different places and times. These fits were made prior to the OPC corrections proposed by Kovilakam and Deshler (2015) and Deshler et al. (2018). These APFs are used in the computation of the limb radiances, which are then compared to the measured radiances to retrieve the aerosol extinction coefficients. As a result, the retrieved aerosol extinction is related to the $P_a(\Theta)$ employed in the retrieval process. The shape of the $P_a(\Theta)$ varies considerably with particle size and refractive index. Thus for spherical sulfuric acid droplets in the stratosphere with a known refractive index, as the particle size increases, the shape of the $P_a(\Theta)$ changes from a simple Rayleigh symmetric phase function to a more complex one with more forward scattering (Boucher, 1998).

Atmos. Meas. Tech. Discuss., https://doi.org/10.5194/amt-2019-119
Manuscript under review for journal Atmos. Meas. Tech.
Discussion started: 12 April 2019

Atmospheric Measurement Techniques Discussions

A long historical record of stratospheric aerosol monitoring is available from the Stratospheric Aerosol and Gas Experiment (SAGE) solar occulation (SO) data. This measurement technique was began by the Stratospheric Aerosol Measurement (SAM) and then the SAGE series that provided a continuous data record (Russell and McCormick, 1989; McCormick and Veiga, 1992; Thomason et al., 1997). SAGE SO data provides a weak constraint on the ASD through the wavelength dependence of the retrieved aerosol extinction, but cannot be used uniquely to correct the ASD (Yue, 1999; Thomason et al., 2008). Due to the lack of global ASD information, different groups have used various techniques to model the $P_a(\Theta)$. One technique that has been used to model the $P_a(\Theta)$ is by computing it based on the parameters of the Henyey-Greenstein (H-G) phase function (Ernst, 2013; Grams, 1981). The shortcomings of using this function to approximate the phase function were demonstrated by Toublanc (1996), who compared the Mie phase function with H-G and modified H-G phase functions for mono-disperse particles and found out that even if the particles were assumed to be spherical, the angular scattering properties could not be approximated to the real phase function with sufficient accuracy if high precision calculations of the phase function was required.

The OSIRIS version 5 (Bourassa et al., 2007) and the OMPS version 0.5 (Loughman et al., 2015; DeLand et al., 2016) aerosol extinction retrievals use a single-mode lognormal ASD to model $P_a(\Theta)$, by using the median radii (r_m) and widths (σ) given in Table 1. For both algorithms, $P_a(\Theta)$ does not vary with altitude or location. (Note that the recently developed V1 (Loughman et al., 2018) and V1.5 (Chen et al., 2018) OMPS aerosol extinction retrieval use updated bi-modal lognormal and gamma phase functions respectively). The Angström exponent (AE) is computed using Equation (1), where K_{ext} is the aerosol extinction coefficient for a particular wavelength.

$$AE = \frac{-ln[K_{ext}(\lambda_1\mathrm{nm})/K_{ext}(\lambda_2\mathrm{nm})]}{ln[\lambda_1\mathrm{nm}/\lambda_2\mathrm{nm}]} \quad (1)$$

Table 1. Lognormal size distribution parameters used to calculate the aerosol phase functions of OMPS V0.5 and OSIRIS v5. The Ångström exponent (AE) is derived from Equation (1) using the 525 nm and 1020 nm extinction coefficients (Nyaku, 2016).

Instrument (Data Version)	$r_m(\mu m)$	σ	AE
OMPS (V0.5)	0.06	1.73	2.34
OSIRIS (V5)	0.08	1.60	2.44

Comparison of the extinction coefficients derived from OPC measurements and SAGE II occultation have shown differences that vary by more than 50% depending on altitude and for a volcanic period and less that 50% on the average for non-volcanic periods (Kovilakam and Deshler, 2015). Also Rieger et al. (2018) have shown that the differences in the lognormal parameters can induce errors of 30% in the aerosol extinction retrievals for OSIRIS geometries and 50% for SCIAMACHY geometries when the correct AE is used. These analyses illustrate the importance of the assumed value of $P_a(\Theta)$ for LS retrievals of K_{ext}, and the limitations of using AE alone to estimate the value of $P_a(\Theta)$.

Atmos. Meas. Tech. Discuss., https://doi.org/10.5194/amt-2019-119
Manuscript under review for journal Atmos. Meas. Tech.
Discussion started: 12 April 2019


Atmospheric Measurement Techniques Discussions

This paper seeks to first show the differences that arise in the computed $P_a(\Theta)$ when different size distribution functions are fitted to the same aerosol concentration measurements. The sensitivity of the derived $P_a(\Theta)$ value to the presence or absence of aerosol concentration information in the aerosol size range of 0.01 μm and 0.1 μm is also explored. Section 2 briefly describes some of the ASDs that have been used in the past to characterize the stratospheric aerosol load and a description of the ASD that is derived from aerosol concentration based on measurements from Laramie, Wyoming optical particle counter (OPC) measurements using balloon-borne instruments (Deshler et al., 2003; Ward et al., 2014). Section 3 focuses on a study which is based on the 2008 - 2017 OPC data at the same location by comparing the unimodal lognormal (UMLN) and the gamma distribution fits to this data set. This is done by concentrating on two altitudes 20 km and 25 km and noting the differences between the phase functions and the Angström exponents of these distributions. The two distributions are then compared to the model outputs of the Community Aerosol and Radiation Model for Atmospheres (CARMA) sectional aerosol microphysics module running online in the NASA Goddard Earth Observing System (GEOS) model. We conclude with a summary and recommendations on which distribution to choose depending on what kind of stratospheric aerosol measurements are available.

2 Aerosol Size Distribution

The aerosol size distribution or the particle number density per unit radius is a statistical model used to describe an ensemble of particles. A number of particle distributions such as the Junge power-law (Junge, 1963), the modified gamma (Deirmendjian, 1969) and up to seven lognormal (Davies, 1974) distributions have been used in the past to represent the distribution of aerosols in the atmosphere. A comprehensive description and a comparative presentation of these distributions is given by (Deepak and Box, 1982) or (Hinds, 1982).

For the characterization of aerosols in the stratosphere, lognormal (LN) size distributions are commonly used, although other distributions have been tried in the past (Rosen and Hofmann, 1986; Sparc, 2006). A discussion of fitting LN distributions to the aerosol measurements obtained from OPC is given by Horvath et al. (1990). LN aerosol size information for stratospheric aerosols has also been been retrieved from LS measurements (Rault and Loughman, 2013; Rieger et al., 2014; Malinina et al., 2018). The UMLN distribution consists of three parameters: The total aerosol concentration and two parameters that indicate the median radius and width of the ASD. The bimodal lognormal (BMLN) distribution became the favored function for fitting stratospheric aerosol concentration measurement since the eruption of Mount Pinatubo injected enormous quantities of sulfur dioxide (SO_2) into the stratosphere (Deshler et al., 2003). This led to the model of coexisting "nucleation" and "accumulation" modes, with the former being associated with new particle formation from sulfur vapor and the latter associated with particle growth by condensation of the vapor on the existing particles (Steele and Turco, 1997).

Since 1991, in-situ stratospheric aerosol concentration measurements using OPCs at Laramie, Wyoming, USA (41°N) at altitudes up to 30 km have been made with 8 and 12 channel instruments, in contrast to the two channel instruments used earlier (see Table 1 of Deshler et al. (2003) for the complete measurement history). The data since 1991 are fit with either unimodal or bimodal lognormal size distributions, depending on which of these distributions minimizes the error with the data.

Atmos. Meas. Tech. Discuss., https://doi.org/10.5194/amt-2019-119
Manuscript under review for journal Atmos. Meas. Tech.
Discussion started: 12 April 2019


Atmospheric Measurement Techniques Discussions

When a second mode is apparent in the data, it generally represents those particles which are moving from the accumulation mode to the coarse mode, and thus is more common at lower altitudes.

2.1 ASD from Wyoming OPC measurements

Stratospheric aerosol measurements have been taken at Laramie, Wyoming since 1971 with the use of an OPC which was originally developed by Rosen (1964) and then modified by Hofmann and Deshler (1991). The instrument measures the intensity of scattered white light at 25° and 40° in the forward direction from single particles passing through the light beam which is larger than the air sample stream. Mie theory is used to determine aerosol size from the amount of the scattered light. The size resolved OPC number concentration measurements are then fitted with an assumed functional form for the size distribution to describe the measurements. The measured concentrations are fitted by either a UMLN or a BMLN size distribution at each measured altitude, where the particle concentrations at distinct size bins are fitted with the function defined by Equation (2) (Deshler et al., 1993, 2003), where the sum is either over $n = 1$ or 2 modes.

$$N(>r) = \sum_{i=1}^{n} \int_{r}^{\infty} \frac{N_i}{\sqrt{2\pi} ln\sigma_{mi}} \exp\left(\frac{-ln^2[x/r_{mi}]}{2ln\sigma_{mi}}\right) d\, lnx \tag{2}$$

This distribution assumes that the measured concentrations are normally distributed with respect to the logarithm of the radius. While the OPCs in use since 1991 employ 8 or 12 aerosol channels, the number of usable measurements decreases as the concentration of the larger particles decreases below detection thresholds. A minimum of four size resolved concentration measurements are required to fit a bimodal distribution. The fifth measurement is obtained from the measurement of the total aerosol population using a condensation nucleus counter (Campbell and Deshler, 2014). The sixth measurement is obtained from the first channel with no aerosol counts, providing the an upper limit on the aerosol concentration at that size. Thus, for every mode of the lognormal distribution, N_i represents the total number concentration, r_{mi} is the median radius, and σ_{mi} is the mode width. $N(>r)$ is the concentration of all particles larger than the lower integration limit, r, and it is the quantity measured by the OPCs. The best fit is the distribution (BMLN or UMLN) which minimizes the root mean square error with respect to the measurements (Deshler et al., 2003; Kovilakam and Deshler, 2015). Measurement uncertainties have been shown to produce errors associated with the variation of air sample flow rate, Poisson counting statistics, and the ability to duplicate the measurements from two identical instruments. These uncertainties have been approximated to be $\pm 30\%$ for size distribution parameters and $\pm 40\%$ for the aerosol moments (Deshler et al., 2003). A systematic calibration error affecting the counting efficiency of the instruments was described by Kovilakam and Deshler (2015). The discovery of this error has led to a modification in the fitting algorithm described in Deshler et al. (2003), such that now an explicit counting efficiency is included in the derivation of the lognormal size distribution fitting parameters (Deshler et al., 2018).

However, during background stratospheric aerosol conditions, OPC measurements may not provide sufficient information about smaller particles ($r < 0.15$ μm) to determine a robust BMLN fit as shown in a recent study to improve OMPS/LP aerosol retrievals by Chen et al. (2018). In that study, Chen et al. (2018) compared four BMLN fits to the same OPC data at 20km altitude (made on 12 April 2000), all having a similar AE of approximately 2.4, but each with a different coarse mode fraction

Atmos. Meas. Tech. Discuss., https://doi.org/10.5194/amt-2019-119
Manuscript under review for journal Atmos. Meas. Tech.
Discussion started: 12 April 2019


Atmospheric Measurement Techniques Discussions

(CMF). These four BMLN distribution fits to the OPC data differed significantly from each other in the radius range between 0.01μm to 0.1μm and these differences resulted from the gaps in the OPC size bins that limited the ability of the fits to be constrained. Consequently, the different ASDs produced $P_a(\Theta)$ that differed significantly form each other as shown in Figure A2 of Chen et al. (2018). Additionally, the BMLN distribution which is defined by 5 parameters (the CMF, 2 median radii, and 2 mode widths) that are independent of each other at each altitude cannot generally be determined in cases where the measurements have less than 5 data points (Malinina et al., 2018). This disparity is further explored in the next section through the reexamination of the OPC data by fitting 2 single mode distributions to the concentration measurements and using only data available since 2008 that has a measurement between the 0.05 μm and 0.1 μm range.

3 Reanalysis of OPC size distribution fits

For a reanalysis of the OPC measurements, it was assumed the stratospheric aerosol could be described by a unimodal distribution during the non-volcanic period under consideration (2008-2017). Either a lognormal or a gamma model is used for which the number of degrees of freedom is reduced from five to two for a normalized distribution during the fitting process (described in Section 3.1). The normalization of the concentrations has no effect on the computation of the APF and the Angström exponent for this study. The choice of these two unimodal distributions is due to their similarity in appearance (Cho et al., 2004). The goodness of the fits is determined by the minimization of the chi-square (χ^2) test statistic. This method estimates the parameters of the fitted distribution by minimizing the difference between the hypothesized and observed distributions. If the data are grouped into k categories (i =1, 2, 3, ..., k) of radii size, the observed frequency in each class is denoted by O_i, and the expected probability from the hypothesized distribution by ζ_i, then the χ^2 value can be calculated from Equations (3 and 4), corresponding to Equation (5.14) described by Wilks (2011)

$$\chi^2(\xi) = \sum_{i=1}^{k} \frac{[O_i - n\zeta_i(\xi)]^2}{n\zeta_i(\xi)} \tag{3}$$

and

$$n = \sum_{i=1}^{k} O_i. \tag{4}$$

To minimize the χ^2 value, the parameters (ξ) of the hypothesized distribution ζ are adjusted until the χ^2 value closest to zero is obtained (Cho et al., 2004). Thus, if the fitted distribution is closer to the distribution of the data, the expected number of particles and the observed number of the particles are very close for each radii range and the square of the differences in numerator of Equation (3) would be very small, leading to a small χ^2 (Wilks, 2011).

To assess whether the number of particles is being over or under estimated between the 0.05 μm and 0.1 μm radii range, data that includes a measurement within this range should be used, but such measurements are not always available. Generally,

Atmos. Meas. Tech. Discuss., https://doi.org/10.5194/amt-2019-119
Manuscript under review for journal Atmos. Meas. Tech.
Discussion started: 12 April 2019

Atmospheric Measurement Techniques Discussions

in-situ OPC aerosol concentration measurements include all particles whose radii are greater than 0.01 μm and size resolved concentrations for particles with radii greater than 0.15 μm and typically up to 2.0 μm in 12 size classes. Beginning in 2008 the OPC development in the late 1980s (Hofmann and Deshler, 1991) was replaced with a new laser based OPC, or LPC (Ward et al., 2014), which is sensitive to particles from 0.094 to 2.0μm radius in 8 size classes. On certain occasions, between 2008 and 2010, there were measurements from both the older OPC and the newer LPC deployed on the same balloon. Further analysis and discussions will explore the importance of this additional bin by comparing the fits that include this bin (called LPC-like herein) to those that were fitted excluding this bin (called OPC-like herein), as well as the resulting phase functions derived from the fits in section 3.2.

3.1 Unimodal lognormal or gamma distribution

Aerosol concentration measurements from Laramie, Wyoming that have been revised following (Kovilakam and Deshler, 2015; Deshler et al., 2018) and measurements with the LPC are used for the current study because of the inclusion of a measurement between 0.05 μm and 0.1 μm. The LPC data consists of 20 months of measurements as shown in Table 2 made from 2008 to 2017 that are fitted with the cumulative forms of the normalized UMLN distribution and the gamma distribution. These data are available from ftp://cat.uwyo.edu/pub/permanent/balloon/Aerosol_InSitu_Meas/US_Laramie_41N_105W/. The normalized form of the cumulative UMLN is obtained by setting N_i of Equation (2) to one and the cummulative gamma distribution is given by Equation (5).

$$F(x,\alpha,\beta) = \int_0^x f(u;\alpha,\beta)du \ = \frac{\gamma(\alpha,\beta,x)}{\Gamma(\alpha)} \tag{5}$$

In the case of the cumulative gamma distribution, $\gamma(\alpha,\beta,x)$ is the lower or incomplete gamma function, where α is the shape parameter and β is the rate parameter. The mean and variance of this distribution are respectively given by $\alpha\beta$ and $\alpha\beta^2$. This distribution can display many shapes by altering the values of α and β, and the pliable shape of this distribution makes it a good candidate for representing stratospheric aerosol data. A difficulty with this distribution as stated by Wilks (2011) is that it is more tedious to work with the gamma distribution, because the two parameters do not correspond exactly to physical parameters representative of the number size distribution of the sampled data, as is the case for the lognormal distribution.

Atmos. Meas. Tech. Discuss., https://doi.org/10.5194/amt-2019-119
Manuscript under review for journal Atmos. Meas. Tech.
Discussion started: 12 April 2019

Atmospheric Measurement Techniques Discussions

Table 2. Table showing the year and the months on which the LPC data was included in this study.

Year	Month
2008	October
2009	January June November
2010	March June
2011	March June July
2012	January March May July September November
2013	March May August October
2014	March July September November
2015	January
2016	April
2017	November

The two altitudes, 20 km and 25 km are chosen to represent two differing aerosols loads well away from the tropopause. For the new fits, the measurements for each aerosol radius bin size which are reported as cumulative number concentrations (N_i) are first normalized to the total aerosol concentration N_0. This value represents the total number concentration and is obtained at the lowest integration limit of 0.01$\mu\mathrm{m}$. After the normalization, bins that have quantities less than 1×10^{-6} are omitted because this number is less than the smallest count distinguishable by the instrument used to make the measurements which is $\sim 10^{-5}$ cm^{-3} (Deshler et al., 2003). The best fit (for which the χ^2 is minimized) is then chosen as the fit for that particular distribution. Examples of the refitted cumulative UMLN and the gamma distributions to the OPC data for the two altitudes are shown in Figure 1 for the June 2010 data. These figures also display for each fit the AE that was computed using Equation (1), where λ_1 and λ_2 are 525 nm and 1020 nm respectively.

To determine which of the two distributions was a better fit to the available data of each month's measurements, a statistical significance test was conducted by using the χ^2 goodness of fit test. This was done such that the null hypothesis H_o stated that: for each measurement the data was drawn from either a UMLN or a gamma distribution. The χ^2 is used as the test statistic with the degrees of freedom v given by Equation (6).

$$v = Number\ of\ measured\ bins - 2 - 1 \tag{6}$$

The number 2 in this equation represents the two parameters (r_m and σ, α and β, for the UMLN or the gamma, respectively) that are fitted for each distribution. The $percentile$ value is defined as the distinct probability that the observed value of the test statistic will occur according to the null hypothesis. Subsequently, the null hypothesis is rejected if the percentile value is less than or equal to the test level and it is not rejected otherwise (Wilks, 2011). A complete summary of the percentile values computed for each of the two altitudes for all the data considered in comparing the two distributions is given in Figure 2.

Atmos. Meas. Tech. Discuss., https://doi.org/10.5194/amt-2019-119
Manuscript under review for journal Atmos. Meas. Tech.
Discussion started: 12 April 2019


Atmospheric Measurement Techniques Discussions

Results from this figure indicate that at both altitudes 20 km and 25 km, the null hypothesis is not rejected at the 15% test level. This signifies that at this level of significance both the UMLN and the gamma distributions are good fits to the data, but at a 5% test level, the null hypothesis is rejected in favor of the alternate hypothesis that the data is taking from a UMLN distribution. Thus, the UMLN distribution is the better of the two distributions that were fitted to the data for the two altitudes that were used in this study.

The fitted parameters are then used to derive the phase functions which are compared among the two distributions. The phase functions derived from the parameters of both distributions compare well to within 10% of each other for scattering angles greater than 20° because the fits of the two distributions overlap. Example of the phase functions derived using the 675 nm wavelength using the UMLN and the gamma distributions fitted parameters displayed in Figure 1 are shown in Figure 3. The shape of the phase functions has been observed to depend on magnitude of the median radius (r_m) in the case of the UMLN distribution and the shape parameter(α) in the case of the gamma distribution. As the magnitude of these two parameters decreases, the resulting phase functions produced from either of the distributions would more closely resemble a Rayleigh phase function as is shown by both distributions in Figure 3 for June 2010 altitude 25 km when the parameters at this altitude are compared with those of June 2010 altitude 20 km. Also, the overlapping behavior observed between the $P_a(\Theta)$ of each of the two distributions at both altitudes shown in Figure 3 is due to the inclusion of a measurement at $\approx$ 0.1 $\mu\mathrm{m}$ and its absence leads to large differences shown later. Phase functions derived from the same dataset but using different fitting models differ from each other and this is a very important issue in the interpretation of measurements from scattering instruments. This is further compounded especially for limb scattering instruments due to multiple scattering effects, since errors in the phase functions produce reflectivity and altitude dependent errors in derived extinctions (Chen et al., 2018).

The AE computed from the parameters of UMLN distribution fits to data are similar those computed from the gamma distribution fitted parameters for the same altitude, as is shown in Figure 4. Moreover, a large AE corresponds to a small median radius in the case of the UMLN distribution or to a small shape parameter in the case of the gamma distribution.

Atmos. Meas. Tech. Discuss., https://doi.org/10.5194/amt-2019-119
Manuscript under review for journal Atmos. Meas. Tech.
Discussion started: 12 April 2019

Atmospheric Measurement Techniques Discussions

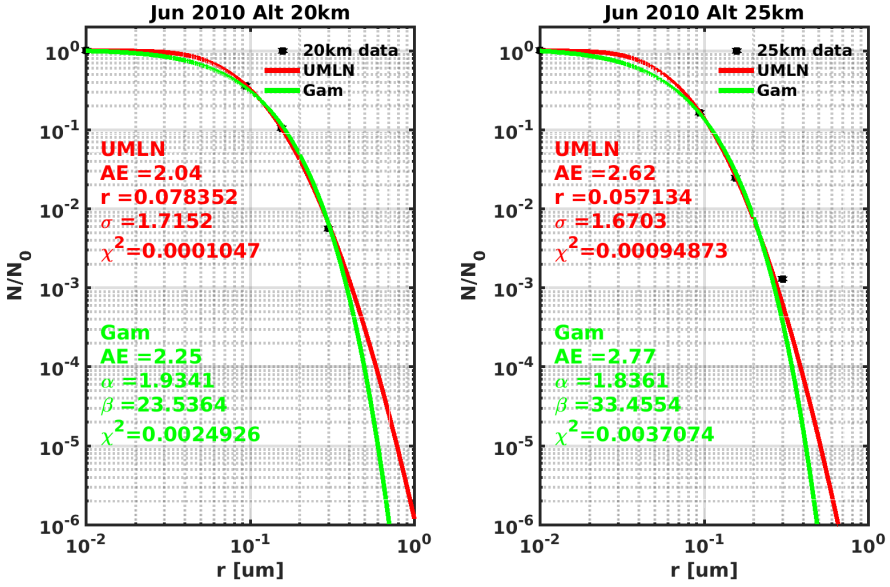

Figure 1. Examples of fitting the UMLN (red line) and gamma (green line) fits to the June 2010 OPC data at altitudes 20 km (left) and 25 km (right) using the minimum χ^2 technique. The figures also show the results of each fit, the minimized χ^2 and the Angström exponent derived from the fitted parameters.

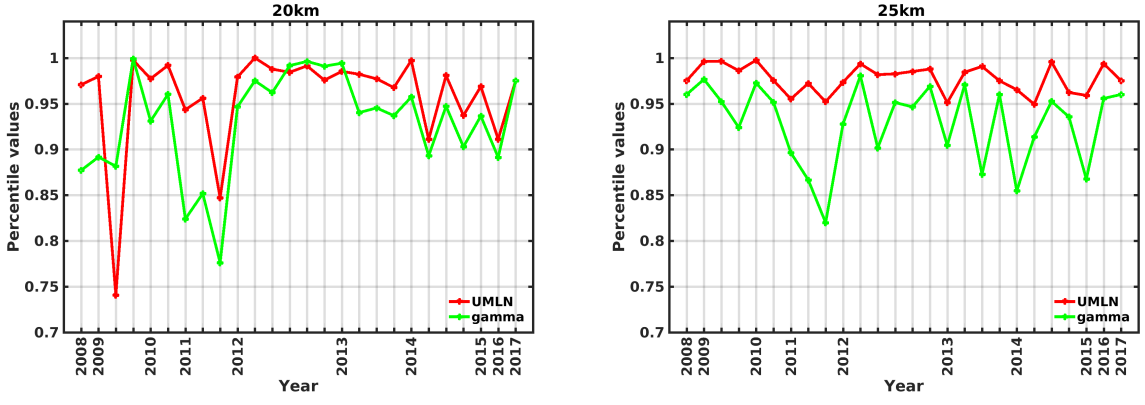

Figure 2. Percentile values computed for the χ^2 values of the UMLN (red line) and gamma (green line) distribution fits to 2008 to 2017 OPC data for altitudes 20 km (left) and 25 km (right).

Atmos. Meas. Tech. Discuss., https://doi.org/10.5194/amt-2019-119
Manuscript under review for journal Atmos. Meas. Tech.
Discussion started: 12 April 2019

Atmospheric Measurement Techniques Discussions

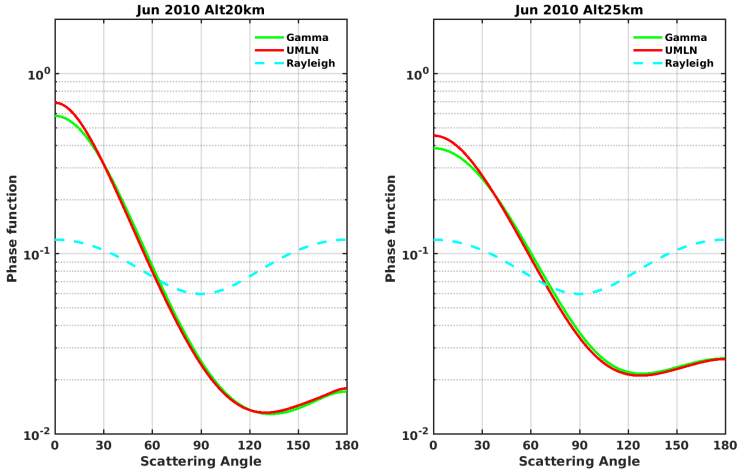

Figure 3. Phase functions derived at 675 nm using the fits shown in Figure 1 for June 2010. The figures correspond to altitude 20 km (left) and to altitude 25 km. (right)

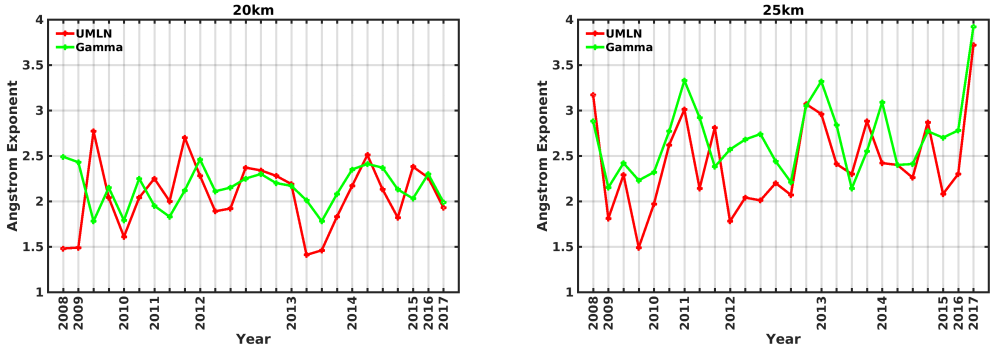

Figure 4. Computed Angström exponents for both the UMLN (red lines) and the gamma (green lines) distribution at altitude 20 km(left) and 25 km (right). Generally, the magnitudes of AEs derived from the gamma distribution are similar to those obtained from the UMLN distribution.

3.2 Importance of a measurement between 0.05 µm and 0.1 µm

The form of $P_a(\Theta)$ for a particular aerosol is determined by the value of the size parameter X, which is the ratio of the aerosol circumference to the wavelength of interest ($X = \frac{2\pi r}{\lambda}$). OMPS V1 aerosol extinctions retrievals are done using the 0.675 µm wavelength, and so the phase function is particularly sensitive to aerosols with radius approximately 0.1 µm (making $X \approx 1$). This is shown in Figure 5, where one observes a considerable change in the magnitude of the phase function, especially in the back-scattering directions ($\Theta \geq 90°$) for this X value. When there are no measurements between the 0.01 and 0.15 µm bin sizes, then the particle concentration within this range is estimated by the function used to fit the data. Errors in estimating the

Atmos. Meas. Tech. Discuss., https://doi.org/10.5194/amt-2019-119
Manuscript under review for journal Atmos. Meas. Tech.
Discussion started: 12 April 2019

Atmospheric Measurement Techniques Discussions

number of particles within this range by the function used for fitting the data will therefore lead to uncertainties in the phase function. The additional 0.094 µm bin in the LPC will augment the measurements.

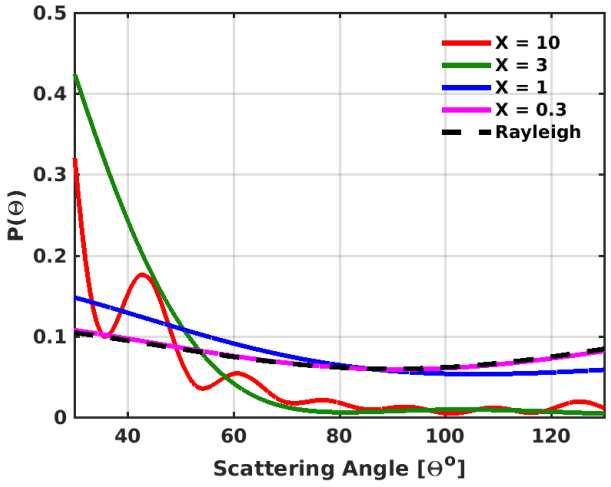

Figure 5. Mie phase functions for different values of the size parameter X derived with a refractive index of 1.33. Observe the increasing asymmetry and complexity of the phase functions with increasing X. The phase functions are shown for the range of scattering angles that are observed by OMPS and OSIRIS.

To show the differences that occur in the fitted distributions, the fits shown in Figure 1 are repeated for each of the two distributions, this time excluding the 0.094 µm bin (to create an "OPC-like" fit) and comparing the phase functions at each altitude. A typical fit showing how the two distributions performed is shown in Figure 6 for June 2010 data at altitude 25 km. The topmost panels shown in Figure 6 indicate that for the OPC-like fits, the UMLN distribution tends to underestimate the measured concentration at the 0.094 µm bin position, whereas the same behavior is not seen with the gamma distribution. The deviations between the fits of the UMLN distribution tend to increase depending on where a measurement bin at the radius $r \approx 0.1$ µm of either the LPC-like or the OPC-like measurement is placed. Thus, the further away a measurement is positioned from $r = 0.1$ µm, the greater the differences observed in the UMLN distribution fits. Also included in this figure are the phase functions (middle plots) determined for the 675 nm wavelength from the fitted parameters of both distributions and the corresponding phase function ratios (bottom plots) of the LPC-like and the OPC-like measurements. Changes of up to $\pm 30\%$ depending on the scattering angle are seen between the derived UMLN distribution phase functions comparison, whereas changes of up $\pm 10\%$ are observed for the derived gamma distribution phase function comparison. The conclusion drawn from this comparison is that the phase functions calculated with the gamma distributions are less sensitive to the radius $r \approx 0.1$ µm observation than the UMLN distribution.This signifies the robustness of the gamma distribution when performing fits on measurements that are made without an intermediary bin between 0.05 µm and 0.1 µm.

Atmos. Meas. Tech. Discuss., https://doi.org/10.5194/amt-2019-119
Manuscript under review for journal Atmos. Meas. Tech.
Discussion started: 12 April 2019

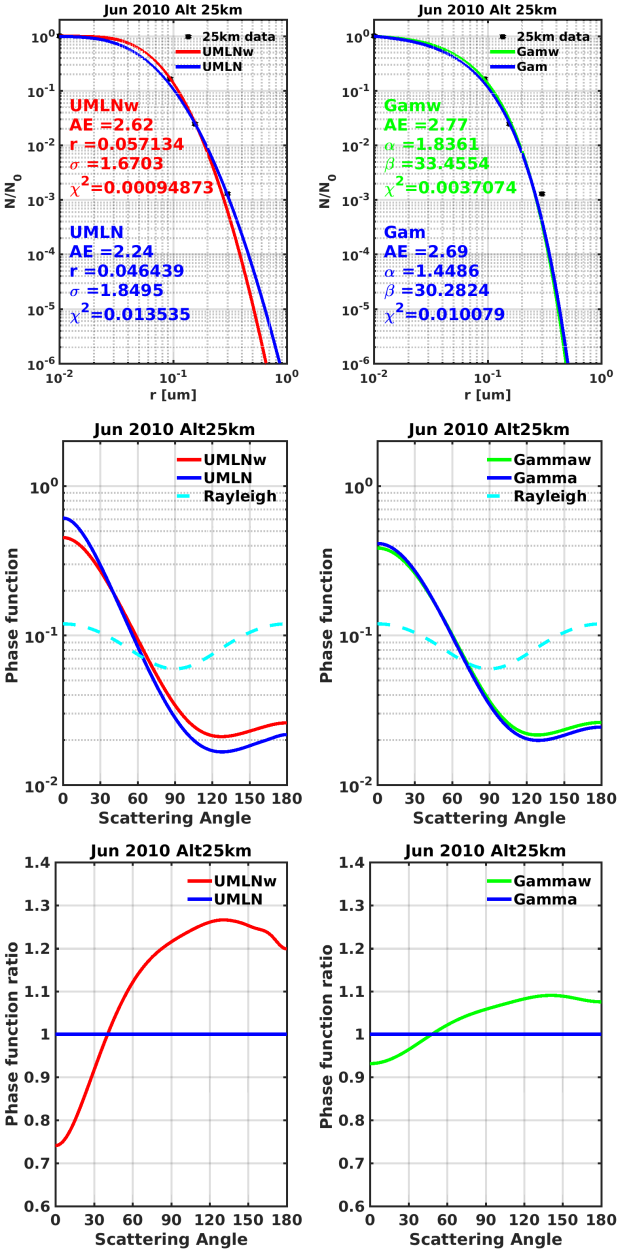

Figure 6. Unimodal lognormal distribution fits (top left) and gamma distribution fits to June 2010 data for altitude 25 km. Blue lines indicate fits made without the 0.094 μm measurement (for an "OPC-like" fit) for both distributions, while the red line fit includes all measurements (for a "LPC-like" fit). The middle figures are the phase functions derived at 675 nm wavelength from the parameters of the fits and the bottom figures show the ratio of the phase functions of LPC-like to OPC-like.

Atmos. Meas. Tech. Discuss., https://doi.org/10.5194/amt-2019-119
Manuscript under review for journal Atmos. Meas. Tech.
Discussion started: 12 April 2019

Atmospheric Measurement Techniques Discussions

3.3 Comparison to the CARMA microphysical model results at Wyoming

The Community Aerosol and Radiation Model for Atmospheres (CARMA) is a general-purpose sectional microphysics code, which was derived from a one-dimensional stratospheric aerosol code that was developed by (Turco et al., 1979; Toon et al., 1979, 1988) to study aerosols and clouds in planetary atmospheres (Hartwick and Toon, 2017). This model includes both aerosol microphysics and gas phase sulfur chemistry that has been described by (English et al., 2011). CARMA has been implemented in the NASA Goddard Earth Observing System (GEOS) Earth system model (Rienecker et al., 2008; Colarco et al., 2014) and configured for modeling stratospheric aerosols similar to English et al. (2011). The ASD is not defined by a statistical distribution but instead is handled using a number of discrete size bins, where the model transport processes are allowed to affect each size bin independently (Rienecker et al., 2008; Colarco et al., 2014). The APF produced by this model is computed directly using the outcome of each discrete bin to perform Mie calculations. The current configuration of this model employs 22 size bins ranging from 0.2 nm to 3.25 $\mu\mathrm{m}$ at 72 vertical levels from the surface of the Earth up to 85km. The model output for this comparison is the June-July-August (JJA) climatology that was averaged at Laramie, Wyoming. The atmosphere contains the background stratospheric aerosol layer, precursor emissions for anthropogenic sulfates and degassing volcanoes that are not explosive in nature. The evolution of particles for this model arises from the condensation of sulfuric acid into aerosols, coagulation and the uniform seeding of sulfuric acid gas. The cumulative UMLN size distribution and the cumulative gamma distribution are then fitted to the model results at selected altitudes between 19 and 26 km using Equations (2) and (5) respectively.

The cumulative distributions fits are performed according to the methodology described in section 3.1 and using selected radii bins in conformity to the size resolved OPC measurements. The results are then validated using the information of all the model bin sizes within the 0.01 $\mu\mathrm{m}$ to 1 $\mu\mathrm{m}$ range. The fitted distributions on the model outputs are shown in Figure 7 for altitudes between 19 km and 26 km. Here, the minimized chi-squares of each fit are computed to include all the bins that were omitted during the fitting process. Comparing the magnitudes of the minimized χ^2 values between the two fitted distributions, the gamma distribution provides a better fit to the normalized CARMA model output at all altitudes that were considered in this study. Figure 7 illustrates the difficulties of a UMLN size distribution, which has the tendency to be too wide, and is one of the reasons why generally bimodal distributions have been found to do a better job in representing the OPC data (Deshler et al., 2003) when there are enough measurements. The gamma distribution does not have the same tendency to overestimate the larger particles. This is confirmed by performing a χ^2 statistic test as to which of these two distribution was a better fit to this model results. The conclusion drawn from the computed percentile values that are shown in Figure 8 that at each altitude considered, the gamma distribution is the best fit to the CARMA model results. The relative differences (RD) computed as percentages using Equation (7) between the phase functions derived from the UMLN P_u and the gamma P_g fits show differences of up to $\pm 15\%$ at 19.85 km to $\pm 50\%$ at 25.60 km at different scattering angles as shown in Figure 9. This

Atmos. Meas. Tech. Discuss., https://doi.org/10.5194/amt-2019-119
Manuscript under review for journal Atmos. Meas. Tech.
Discussion started: 12 April 2019

implies that different distributions applied to the same data set would produce phase functions that differ greatly from each other at various scattering angles.

$$RD\ (\%) = \left(1 - \frac{P_u}{P_g}\right) \times 100\% \tag{7}$$

Finally, a comparison is made between the mean phase functions derived from OPC data fitted with the UMLN distribution and the CARMA model results fitted with the gamma distribution at altitude 25 km. The mean and the standard deviation of OPC UMLN phase functions are obtained for each angle from the phase functions of all the months of June, July and August (JJA) from 2008 to 2017. Results from this comparison as shown in Figure 10 indicate that the phase function derived from the gamma distribution fit to the CARMA model outputs at Wyoming agrees very well to within one standard deviation of the mean phase function of the JJA UMLN distribution fit to the OPC dataset at this altitude. This agreement between the two phase functions is also shown to be within $\pm 15\%$ at all scattering angles and this reduces to $\pm 5\%$ within the scattering angle range of 15° to 180°. The good comparison shown by the phase function from the CARMA model with that of the OPC dataset at Laramie, Wyoming provides a justification for the use of the CARMA model results at other locations on the Earth and for periods with moderate volcanic activity.

Atmos. Meas. Tech. Discuss., https://doi.org/10.5194/amt-2019-119
Manuscript under review for journal Atmos. Meas. Tech.
Discussion started: 12 April 2019

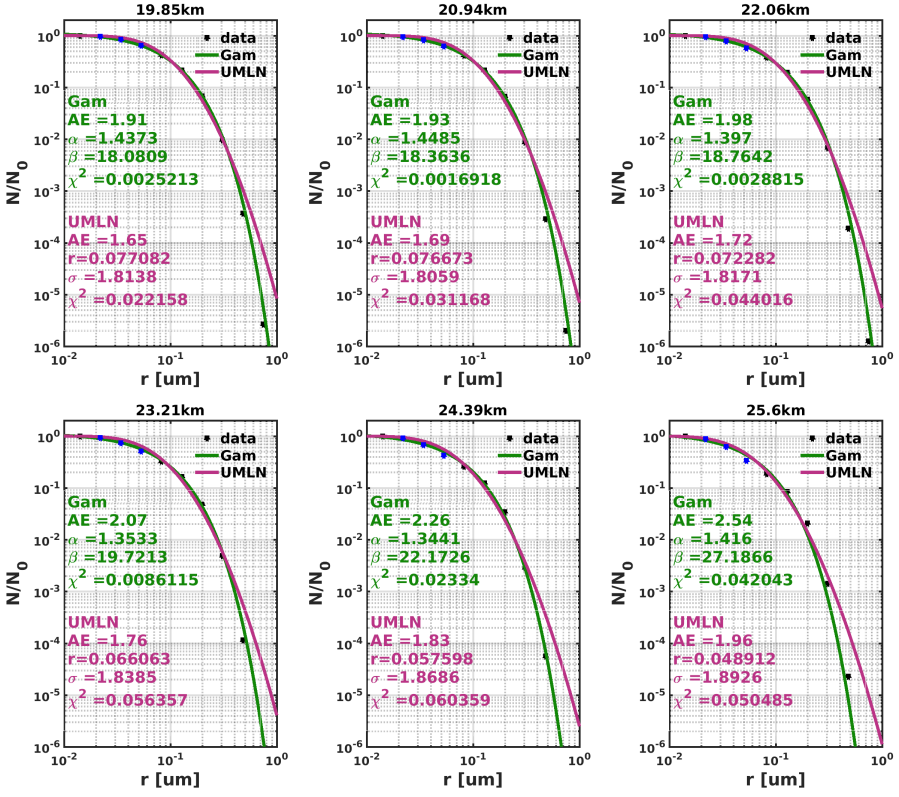

Figure 7. Unimodal lognormal and gamma distribution fits to the normalized CARMA model data. The blue data points are excluded during the fitting procedure, but are included during the validation of the fits. The green lines are the gamma distribution fits and the purple lines are the UMLN distribution fits. The magnitudes of the minimized $\chi^2 s$ among the two distribution indicate that the gamma distribution fits this model data better than the UMLN distribution.

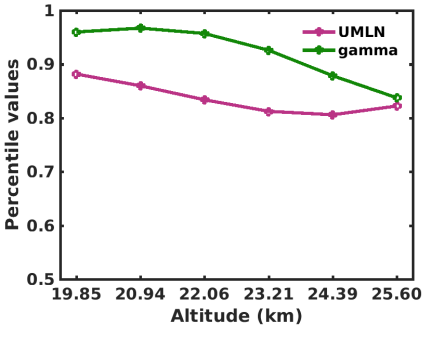

Figure 8. Percentile values computed from the minimized χ^2 of the fits of both the UMLN and gamma distributions to determine the level of confidence for which either distribution is chosen to describe the CARMA model data.

Atmos. Meas. Tech. Discuss., https://doi.org/10.5194/amt-2019-119
Manuscript under review for journal Atmos. Meas. Tech.
Discussion started: 12 April 2019

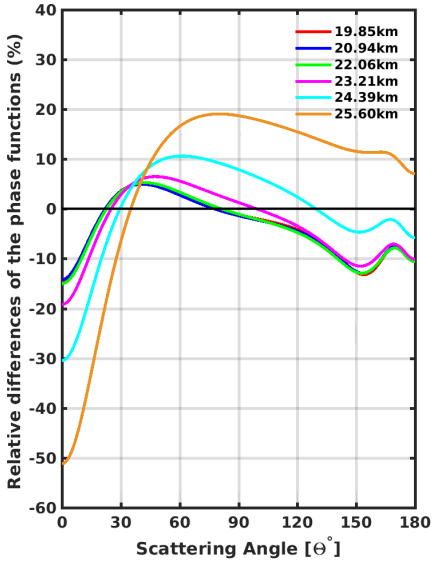

Figure 9. Relative differences between the phase functions derived from the gamma and the UMLN parameters fitted to the CARMA model data at each of the six altitudes from 19.85 km to 25.60 km. The differences between the phase functions are shown to increase as the altitude increases from $\pm 15\%$ at 19.85 km to $\pm 50\%$ at 25.60 km.

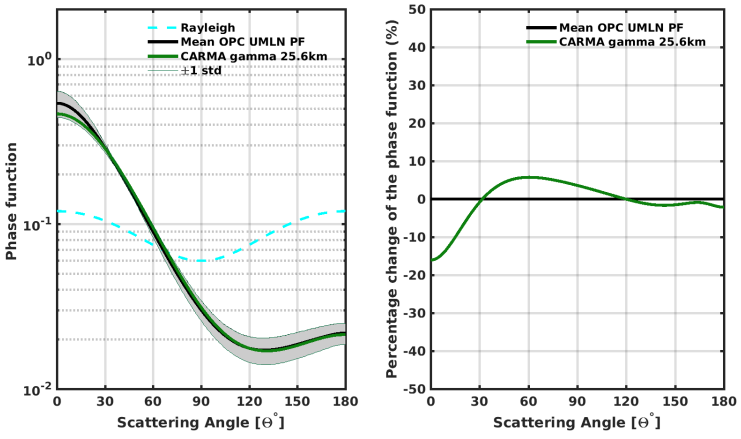

Figure 10. The figure on the left shows the mean and the standard deviation of phase functions derived from the fits of the UMLN distribution for all the OPC data used for the months of June, July and August (JJA) at altitude 25km are compared to the phase function derived from the fit to the CARMA model data at altitude 25.6 km for the wavelength 675 nm. The figure on the right shows the change between the two phase functions to be less than $\pm 15\%$ at all scattering angles.

Atmos. Meas. Tech. Discuss., https://doi.org/10.5194/amt-2019-119
Manuscript under review for journal Atmos. Meas. Tech.
Discussion started: 12 April 2019


Atmospheric Measurement Techniques Discussions

4 Concluding discussions and Summary

Measured limb scattered radiance is sensitive to presence of stratospheric aerosols due to the long path the scattered solar photons have to travel through the aerosol layer to reach the sensor (Loughman et al., 2018; Chen et al., 2018; Rieger et al., 2015). This radiance is not only composed of photons that were singly scattered directly in the along the line of sight (LOS) of the instrument but also includes photons that were scattered multiple times before they were finally scattered into the LOS of the instrument. Along the LOS of the sensor, the scattered radiance is driven not only by the APF but is further attenuated by air molecules and trace gases, making untangling of the information content in these measurements very complicated. Moreover, diffuse upwelling radiation from the lower atmosphere is also scattered and attenuated along the LOS. To unravel the composition of these measurements requires a good knowledge of APF which is derived through the ASD that is assigned to these aerosols, and thus the choice of which theoretical distribution (UMLN or gamma) should be used to describe these particles in the stratosphere is important.

We have investigated fitting a UMLN and a gamma distribution to the 2008 to 2017 LPC measurements for altitudes 20 km and 25 km. The parameters of the distributions were found by minimizing the χ^2 test statistic between the measurements and the theoretical distributions. As a first step, we assumed that the stratospheric aerosol is distributed with a single mode during the background conditions and could be fitted to either of the two distributions. Typically, both the UMLN and the gamma cumulative distributions are found to be good representatives for the stratospheric aerosol concentration measurements made by the University of Wyoming LPC at the two altitudes as was suggested by the χ^2 values. In order to discriminate between them, a χ^2 goodness of fit test applied showed that to a 10% level of confidence the UMLN was the better of the two distributions as it fitted all data at the two altitudes and for all the months of data that were considered.

Additionally, it has been shown that whenever OPC-like concentration measurements are made, the gamma distribution is the best distribution to be fitted to this data since it is more robust and able to predict the amount of particles within the 0.01 $\mu\mathrm{m}$ and 0.1 $\mu\mathrm{m}$ range when compared to the UMLN distribution. This conclusion was drawn from the comparison of the phase functions derived from the two distributions fitted to the LPC data, when measurements are not provided between aerosol size ranges of 0.01 $\mu\mathrm{m}$ and 0.1 $\mu\mathrm{m}$ range by deliberately omitting the 0.094 $\mu\mathrm{m}$ bin and fitting the distributions. This limited analysis indicates that if a single mode ASD is to be assumed then the gamma distribution model provides an improved fit to the University of Wyoming LPC data, and by extension other in situ data, that do not include sizes below 0.1 $\mu\mathrm{m}$ in their measurements. When such small particle measurements are available, however, there is little distinction between the size distributions, if the usefulness of the physical significance of the lognormal size distribution parameters are not included.

A similar analysis was further conducted using data obtained from the aerosol microphysical model, CARMA to ascertain which distribution was the best to represent the background aerosol load in the stratosphere. Again, both distributions fitted these data very well for all the altitudes considered. Quantitative comparisons of the goodness of fit for these unimodal distributions indicated that the gamma distribution does a slightly better job for these comparisons in a volcanically quiescent stratosphere. These kinds of closure studies are very important for the improvement of the confidence levels in space-based data that is used to test aerosol microphysical models and for estimating radiative forcing due to stratospheric aerosols.

The overall implication of this study is to show the importance of the nature of APF used in the retrieval of the stratospheric aerosol extinction from limb scattering measurements. The phase function is derived from either the parameters of the UMLN or the gamma cumulative distributions fitted to LPC measurements and other in situ data which may or may not include a measurement in the aerosol size range of 0.01 μm and 0.1 μm. The fits made by using the UMLN distribution have a tendency to over or under estimate the number of particles within this aerosol size range as compared to fits made using the gamma distribution when no measurements are given within that radii range. This leads to phase functions that may not be a true representation of the measurements. Thus, it is imperative for one to have a knowledge about the nature of the measurements from which the parameters of any distribution are provided. Because of the robustness of the gamma distribution, phase functions are best computed with this distribution for in situ or OPC measurements that do not provide a data point in the aerosol size range of 0.01 μm and 0.1 μm.

Data availability. OPC data is available for download at: ftp://cat.uwyo.edu/pub/permanent/balloon/Aerosol_InSitu_Meas/US_Laramie_41N_105W/.

Competing interests. The authors declare that they have no conflict of interest.

Acknowledgements. This work was supported by NASA GSFC through SSAI Subcontract 21205-12-043. The authors thank NASA and NOAA for supporting limb scattering research, and particularly recognize Didier Rault for years of leadership developing the OMPS LP algorithms. We would also like to thank Matthew DeLand for his support.

References

Andreae, M. O. and Crutzen, P. J.: Atmospheric aerosols: Biogeochemical sources and role in atmospheric chemistry, Science, 276, 1052–1058, 1997.

Boucher, O.: On aerosol direct shortwave forcing and the Henyey-Greenstein phase function, Journal of the atmospheric sciences, 55, 128–134, 1998.

Bourassa, A., Degenstein, D., and Llewellyn, E.: Retrieval of stratospheric aerosol size information from OSIRIS limb scattered sunlight spectra, Atmospheric Chemistry and Physics, 8, 6375–6380, 2008.

Bourassa, A. E., Degenstein, D. A., Gattinger, R. L., and Llewellyn, E. J.: Stratospheric aerosol retrieval with optical spectrograph and infrared imaging system limb scatter measurements, Journal of Geophysical Research D: Atmospheres, 112, 2007.

Bourassa, A. E., Rieger, L. A., Lloyd, N. D., and Degenstein, D. A.: Odin-OSIRIS stratospheric aerosol data product and SAGE III intercomparison, Atmospheric Chemistry and Physics, 12, 605–614, https://doi.org/10.5194/acp-12-605-2012, https://www.atmos-chem-phys.net/12/605/2012/, 2012.

Bovensmann, H., Burrows, J., Buchwitz, M., Frerick, J., Noël, S., Rozanov, V., Chance, K., and Goede, A.: SCIAMACHY: Mission objectives and measurement modes, Journal of the Atmospheric Sciences, 56, 127–150, 1999.

Campbell, P. and Deshler, T.: Condensation nuclei measurements in the midlatitude (1982–2012) and Antarctic (1986–2010) stratosphere between 20 and 35 km, Journal of Geophysical Research: Atmospheres, 119, 137–152, 2014.

Chen, Z., Bhartia, P. K., Loughman, R., Colarco, P., and DeLand, M.: Improvement of stratospheric aerosol extinction retrieval from OMPS/LP using a new aerosol model, Atmospheric Measurement Techniques, 11, 6495–6509, 2018.

Cho, H.-K., Bowman, K. P., and North, G. R.: A comparison of gamma and lognormal distributions for characterizing satellite rain rates from the tropical rainfall measuring mission, Journal of Applied Meteorology, 43, 1586–1597, 2004.

Colarco, P. R., Nowottnick, E. P., Randles, C. A., Yi, B., Yang, P., Kim, K.-M., Smith, J. A., and Bardeen, C. G.: Impact of radiatively interactive dust aerosols in the NASA GEOS-5 climate model: Sensitivity to dust particle shape and refractive index, Journal of Geophysical Research: Atmospheres, 119, 753–786, https://doi.org/10.1002/2013JD020046, 2014.

Davies, C.: Size distribution of atmospheric particles, Journal of Aerosol Science, 5, 293 – 300, https://doi.org/https://doi.org/10.1016/0021-8502(74)90063-9, http://www.sciencedirect.com/science/article/pii/0021850274900639, 1974.

Deepak, A. and Box, G. P.: Representation of aerosol size distribution data by analytic models, in: Atmospheric Aerosols: Their Formation, Optical Properties, and Effects, p. 79, 1982.

Deirmendjian, D.: Electromagnetic scattering on spherical polydispersions, Tech. rep., RAND CORP SANTA MONICA CA, 1969.

DeLand, M., Bhartia, P., Xu, P., and Zhu, T.: OMPS Limb Profiler Aerosol Extinction Product AER675: Version 0.5 Data Release Notes, https://ozoneaq.gsfc.nasa.gov/media/docs/OMPS_LP_AER675_V0.5_Release_Notes.pdf, 2016.

Deshler, T., Johnson, B. J., and Rozier, W. R.: Balloonborne measurements of Pinatubo aerosol during 1991 and 1992 at 41°N: Vertical profiles, size distribution, and volatility, Geophysical Research Letters, 20, 1435–1438, https://doi.org/10.1029/93GL01337, http://dx.doi.org/10.1029/93GL01337, 1993.

Deshler, T., Hervig, M., Hofmann, D., Rosen, J., and Liley, J.: Thirty years of in situ stratospheric aerosol size distribution measurements from Laramie, Wyoming (41 N), using balloon-borne instruments, Journal of Geophysical Research: Atmospheres, 108, 2003.

Deshler, T., Kovilakam, M., Luo, B., Peter, T., and Kalnajs, L.: Retrieval of aerosol size distributions from in situ particle counter measurements accounting for instrument counting efficiency, and comparisons with satellite measurements of extinction and estimates of aerosol surface area, Submitted to Journal of Geophysical Research, 2018.

English, J., Toon, O., Mills, M., and Yu, F.: Microphysical simulations of new particle formation in the upper troposphere and lower stratosphere, Atmospheric Chemistry and Physics, 11, 9303, 2011.

Ernst, F.: Stratospheric aerosol extinction profile retrievals from SCIAMACHY limb-scatter observations, Ph.D. thesis, Staats-und Universitätsbibliothek Bremen, 2013.

Flynn, L., Seftor, C., Larsen, J., and Xu, P.: The Ozone Mapping and Profiler Suite, in: Earth Science Satellite Remote Sensing, edited by Qu, J., Gao, W., Kafatos, M., Murphy, R., and Salomonson, V., pp. 279–296, Springer Berlin Heidelberg, https://doi.org/10.1007/978-3-540-37293-6_15, http://dx.doi.org/10.1007/978-3-540-37293-6_15, 2006.

Grams, G. W.: In-situ measurements of scattering phase functions of stratospheric aerosol particles in Alaska during July 1979, Geophysical Research Letters, 8, 13–14, https://doi.org/10.1029/GL008i001p00013, https://agupubs.onlinelibrary.wiley.com/doi/abs/10.1029/GL008i001p00013, 1981.

Hartwick, V. and Toon, O.: Micrometeoric Ablation Biproducts as a High Altitude Source for Ice Nuclei in the Present Day Martian Atmosphere, in: The Sixth International Workshop on the Mars Atmosphere: Modelling and observation was held on January 17-20 2017, in Granada, Spain. Scientific committee: F. Forget, MA Lopez-Valverde, S. Amiri, M.-C. Desjean, F. Gonzalez-Galindo, J. Hollingsworth, B. Jakosky, SR Lewis, D. McCleese, E. Millour, H. Svedhem, D. Titov, M. Wolff., p. 4103, p. 4103, 2017.

Hinds, W.: Aerosol technology: properties, behavior, and measurement of airborne particles, A Wiley-Interscience Publication John Wiley & Sons, 1982.

Hofmann, D. and Deshler, T.: Stratospheric cloud observations during formation of the Antarctic ozone hole in 1989, Journal of Geophysical Research: Atmospheres, 96, 2897–2912, 1991.

Horvath, H., Gunter, R., and Wilkison, S.: Determination of the coarse mode of the atmospheric aerosol using data from a forward-scattering spectrometer probe, Aerosol Science and Technology, 12, 964–980, 1990.

Jaross, G., Bhartia, P. K., Chen, G., Kowitt, M., Haken, M., Chen, Z., Xu, P., Warner, J., and Kelly, T.: OMPS Limb Profiler instrument performance assessment, Journal of Geophysical Research: Atmospheres, 119, 4399–4412, 2014.

Junge, C. E.: Air chemistry and radioactivity, 1963, p. 382, 1963.

Junge, C. E., Chagnon, C. W., and Manson, J. E.: A world-wide stratospheric aerosol layer, Science, 133, 1478–1479, 1961.

Kovilakam, M. and Deshler, T.: On the accuracy of stratospheric aerosol extinction derived from in situ size distribution measurements and surface area density derived from remote SAGE II and HALOE extinction measurements, Journal of Geophysical Research: Atmospheres, 120, 8426–8447, 2015.

Kravitz, B., Robock, A., Bourassa, A., Deshler, T., Wu, D., Mattis, I., Finger, F., Hoffmann, A., Ritter, C., Bitar, L., et al.: Simulation and observations of stratospheric aerosols from the 2009 Sarychev volcanic eruption, Journal of Geophysical Research: Atmospheres, 116, 2011.

Kremser, S., Thomason, L. W., Hobe, M., Hermann, M., Deshler, T., Timmreck, C., Toohey, M., Stenke, A., Schwarz, J. P., Weigel, R., et al.: Stratospheric aerosol—Observations, processes, and impact on climate, Reviews of Geophysics, 54, 278–335, 2016.

Llewellyn, E. J., Lloyd, N. D., Degenstein, D. A., Gattinger, R. L., Petelina, S. V., Bourassa, A. E., Wiensz, J. T., Ivanov, E. V., McDade, I. C., Solheim, B. H., McConnell, J. C., Haley, C. S., Von Savigny, C., Sioris, C. E., McLinden, C. A., Griffioen, E., Kaminski, J., Evans, W. F. J., Puckrin, E., Strong, K., Wehrle, V., Hum, R. H., Kendall, D. J. W., Matsushita, J., Murtagh, D. P., Brohede, S., Stegman, J., Witt,

G., Barnes, G., Payne, W. F., Piché, L., Smith, K., Warshaw, G., Deslauniers, D. ., Marchand, P., Richardson, E. H., King, R. A., Wevers, I., McCreath, W., Kyrölä, E., Oikarinen, L., Leppelmeier, G. W., Auvinen, H., Mégie, G., Hauchecorne, A., Lefèvre, F., De La Nöe, J., Ricaud, P., Frisk, U., Sjoberg, F., Von Schéele, F., and Nordh, L.: The OSIRIS instrument on the Odin spacecraft, Canadian Journal of Physics, 82, 411–422, 2004.

Loughman, R., Flittner, D., Nyaku, E., and Bhartia, P. K.: Gauss-Seidel limb scattering (GSLS) radiative transfer model development in support of the Ozone Mapping and Profiler Suite (OMPS) limb profiler mission, Atmospheric Chemistry and Physics, 15, 3007–3020, http://www.atmos-chem-phys.net/15/3007/2015/, 2015.

Loughman, R., Bhartia, P. K., Chen, Z., Xu, P., Nyaku, E., and Taha, G.: The Ozone Mapping and Profiler Suite (OMPS) Limb Profiler (LP) Version 1 aerosol extinction retrieval algorithm: theoretical basis, Atmospheric Measurement Techniques, 11, 2633–2651, https://doi.org/10.5194/amt-11-2633-2018, https://www.atmos-meas-tech.net/11/2633/2018/, 2018.

Malinina, E., Rozanov, A., Rozanov, V., Liebing, P., Bovensmann, H., and Burrows, J. P.: Aerosol particle size distribution in the stratosphere retrieved from SCIAMACHY limb measurements, Atmospheric Measurement Techniques, 11, 2085–2100, 2018.

McCormick, M. P. and Veiga, R. E.: SAGE II measurements of early Pinatubo aerosols, Geophysical Research Letters, 19, 155–158, 1992.

McCormick, M. P., Thomason, L. W., and Trepte, C. R.: Atmospheric effects of the Mt Pinatubo eruption, Nature, 373, 399–404, 1995.

Nyaku, E. M.: Characterizing aerosol properties in the upper troposphere and stratosphere from limb scatter radiance, PhD dissertation, Hampton University, Center for Atmospheric Sciences, this is a full PHDTHESIS entry, 2016.

Ovigneur, B., Landgraf, J., Snel, R., and Aben, I.: Retrieval of stratospheric aerosol density profiles from SCIAMACHY limb radiance measurements in the O 2 A-band, Atmospheric Measurement Techniques, 4, 2359–2373, 2011.

Rault, D. and Loughman, R.: Stratospheric and upper tropospheric aerosol retrieval from limb scatter signals, in: Proc. SPIE, vol. 6745, p. 674509, 2007.

Rault, D. F. and Loughman, R. P.: The OMPS limb profiler environmental data record algorithm theoretical basis document and expected performance, IEEE Transactions on Geoscience and Remote Sensing, 51, 2505–2527, 2013.

Ridley, D., Solomon, S., Barnes, J., Burlakov, V., Deshler, T., Dolgii, S., Herber, A. B., Nagai, T., Neely, R., Nevzorov, A., et al.: Total volcanic stratospheric aerosol optical depths and implications for global climate change, Geophysical Research Letters, 41, 7763–7769, 2014.

Rieger, L., Bourassa, A., and Degenstein, D.: Merging the OSIRIS and SAGE II stratospheric aerosol records, Journal of Geophysical Research: Atmospheres, 120, 8890–8904, 2015.

Rieger, L. A., Bourassa, A. E., and Degenstein, D. A.: Stratospheric aerosol particle size information in Odin-OSIRIS limb scatter spectra, Atmospheric Measurement Techniques, 7, 507–522, https://doi.org/10.5194/amt-7-507-2014, http://www.atmos-meas-tech.net/7/507/2014/, 2014.

Rieger, L. A., Malinina, E. P., Rozanov, A. V., Burrows, J. P., Bourassa, A. E., and Degenstein, D. A.: A study of the approaches used to retrieve aerosol extinction, as applied to limb observations made by OSIRIS and SCIAMACHY, Atmospheric Measurement Techniques, 11, 3433–3445, https://doi.org/10.5194/amt-11-3433-2018, https://www.atmos-meas-tech.net/11/3433/2018/, 2018.

Rienecker, M., Suarez, M. J., Todling, R., Bacmeister, J., Takacs, L., Liu, H., Gu, W., Sienkiewicz, M., Koster, R., Gelaro, R., Stajner, I., and Nielsen, J.: The GEOS-5 Data Assimilation System-Documentation of Versions 5.0. 1, 5.1. 0, and 5.2. 0, NASA Technical Report Series on Global Modeling and Data Assimilation, 27, 1–118, 2008.

Robock, A.: Volcanic eruptions and climate, Reviews of Geophysics, 38, 191–219, 2000.

Rosen, J. M.: The vertical distribution of dust to 30 kilometers, Journal of Geophysical Research, 69, 4673–4676, https://doi.org/10.1029/JZ069i021p04673, http://dx.doi.org/10.1029/JZ069i021p04673, 1964.

Rosen, J. M. and Hofmann, D. J.: Optical modeling of stratopheric aerosols: present status, Applied optics, 25, 410–419, 1986.

Russell, P. B. and McCormick, M. P.: SAGE II aerosol data validation and initial data use: an introduction and overview, Journal of Geophysical Research, 94, 8335–8338, 1989.

Solomon, S.: Stratospheric ozone depletion: A review of concepts and history, Reviews of Geophysics, 37, 275–316, 1999.

Sparc: SPARC Assessment of Stratospheric Aerosol Properties, L. Thomason and T. Peter (eds.),SPARC Report No. 4, 2006.

Steele, H. M. and Turco, R. P.: Retrieval of aerosol size distributions from satellite extinction spectra using constrained linear inversion, Journal of Geophysical Research: Atmospheres, 102, 16 737–16 747, https://doi.org/10.1029/97JD01264, http://dx.doi.org/10.1029/97JD01264, 1997.

Taha, G., Rault, D. F., Loughman, R. P., Bourassa, A. E., and Von Savigny, C.: SCIAMACHY stratospheric aerosol extinction profile retrieval using the OMPS/LP algorithm, Atmospheric Measurement Techniques, 4, 547–556, 2011.

Thomason, L., Poole, L., and Deshler, T.: A global climatology of stratospheric aerosol surface area density deduced from Stratospheric Aerosol and Gas Experiment II measurements: 1984–1994, Journal of Geophysical Research: Atmospheres, 102, 8967–8976, 1997.

Thomason, L. W., Burton, S. P., Luo, B.-P., and Peter, T.: SAGE II measurements of stratospheric aerosol properties at non-volcanic levels, Atmospheric Chemistry and Physics, 8, 983–995, 2008.

Toon, O., Turco, R., Westphal, D., Malone, R., and Liu, M.: A multidimensional model for aerosols: Description of computational analogs, Journal of the Atmospheric Sciences, 45, 2123–2144, 1988.

Toon, O. B., Turco, R., Hamill, P., Kiang, C., and Whitten, R.: A one-dimensional model describing aerosol formation and evolution in the stratosphere: II. Sensitivity studies and comparison with observations, Journal of the Atmospheric Sciences, 36, 718–736, 1979.

Toublanc, D.: Henyey–Greenstein and Mie phase functions in Monte Carlo radiative transfer computations, Applied optics, 35, 3270–3274, 1996.

Turco, R., Hamill, P., Toon, O., Whitten, R., and Kiang, C.: A one-dimensional model describing aerosol formation and evolution in the stratosphere: I. Physical processes and mathematical analogs, Journal of the Atmospheric Sciences, 36, 699–717, 1979.

von Savigny, C., Ernst, F., Rozanov, A., Hommel, R., Eichmann, K.-U., Rozanov, V., Burrows, J. P., and Thomason, L. W.: Improved stratospheric aerosol extinction profiles from SCIAMACHY: validation and sample results, Atmospheric Measurement Techniques, 8, 5223–5235, https://doi.org/10.5194/amt-8-5223-2015, http://www.atmos-meas-tech.net/8/5223/2015/, 2015.

Ward, S. M., Deshler, T., and Hertzog, A.: Quasi-Lagrangian measurements of nitric acid trihydrate formation over Antarctica, Journal of Geophysical Research: Atmospheres, 119, 245–258, https://doi.org/10.1002/2013JD020326, http://dx.doi.org/10.1002/2013JD020326, 2013JD020326, 2014.

Wilks, D.: Statistical Methods in the Atmospheric Sciences, vol. 100, Academic Press, 3 edn., 2011.

Yue, G. K.: A new approach to retrieval of aerosol size distributions and integral properties from SAGE II aerosol extinction spectra, Journal of Geophysical Research: Atmospheres, 104, 27 491–27 506, 1999.